Lattice Signal Sets to Combat Pulsed Interference from Aeronautical Signals

Khodr A. Saaifan and Werner Henkel
Transmission Systems Group (TrSyS)
Jacobs University Bremen
Bremen 28759, Germany
{k.saaifan, w.henkel}@jacobs-university.de

Abstract—The inlay approach for the Broadband Aeronautical Multicarrier Communications (B-AMC) system is exposed to severe interference from the adjacent channels of the distance measuring equipment (DME) system. Here, we propose a simple technique to mitigate DME interference and subsequently enable transmission in the spectral gaps of the DME channels. The proposed technique uses a precoding at the transmitter based on employing lattice signal sets in order to modify the shape of the DME signal spectrum. Hereto, a simple clipping method is applied to the received subcarriers to mitigate the impact of the DME interference. Simulations show that the proposed subcarrier clipping technique can considerably reduce the effect of the DME signal by choosing appropriate clipping thresholds. They have been selected to maximize the signal-to interference-and-noise ratio (SINR) after the clipping operation. It has also been confirmed by simulations that the proposed method offers a significantly better performance when compared to current mitigation techniques.

Index Terms—OFDM, multicarrier, impulse noise, pulse clipping, DME, lattice signal set

I. INTRODUCTION

L-DACS1 is a broadband candidate for the future L-band Digital Aeronautical Communications System (L-DACS). Such a system has been proposed by the German Aerospace Center (DLR) to be operating in the L-band. The physical layer of the L-DACS1 system employing Orthogonal Frequency-Division Multiplexing (OFDM) as modulation scheme and Frequency-Division Duplex (FDD) for separating forward (FL) and reverse link (RL).

The aeronautical part of the L-band is mainly used by a DME or a tactical air navigation system (TACAN). These systems are used to determine the slant range between an airborne and a ground station. For an efficient use of bandwidth in the L-band, B-AMC is developed as an inlay system between two adjacent channels used by DME ground stations. There are many challenges for the inlay approach: 1) B-AMC must not disturb the existing L-band system. 2) B-AMC is subject to strong ingress originating from existing L-band systems. Therefore, B-AMC must employ an efficient interference mitigation technique to achieve reliable communication. For reducing out-of-band radiation of the OFDM signal causing interference towards the licensed system, powerful techniques have been proposed in [3]. To mitigate the impact of DME signals, clipping and pulse blanking have been used in the

E5- and L5-bands used by satellite navigation systems [4]. Both approaches have been developed and applied to the B-AMC system [5]. In addition, an erasure-based convolutional decoding strategy has been investigated in [6] to mitigate the impact of DME interference.

In this paper, our proposed DME mitigation techniques are directed towards lattice signal sets realizing modulation diversity [7]. This type of diversity has no detrimental effect on the spectral efficiency. Modulation diversity is obtained by applying fully diverse unitary transformations to inputs drawn from multidimensional digital modulation signals [8]. Here, the advantage of applying a unitary transformation is exploited in order to modify the shape of the DME signal spectrum at the receiver. Based on this transformation, a simple clipping method can be applied efficiently in frequency domain to significantly reduce the impact of interference from the impaired subcarriers.

The rest of the paper is organized as follows. Section II briefly describes the system under consideration. Section III reviews the characteristics of the DME signal. In Section IV, we present the concepts of lattice signal sets, and a suitable lattice code for modifying the spectrum of the DME signal is introduced additionally. In Section V, the proposed subcarrier clipping technique is introduced to reduce the impact of interference. Finally, simulation results and concluding remarks are presented in sections VI and VII, respectively.

II. SYSTEM MODEL

The B-AMC physical layer is the core of L-DACS1 and is based on OFDM modulation and designed to operate in the aeronautical L-band (960 -1164 MHz). A detailed physical layer description including all relevant OFDM parameters is given in [1]. According to these parameters, a bandwidth of 500 kHz is considered to be available for each B-AMC channel (FL or RL), with 48 subcarriers used for data transmission. An FFT of length 64 is used with 8 guard subcarriers on the left and the right side of the spectrum for filtering purposes. The guard interval (cyclic prefix) consumes 20 % of the overall OFDM symbol duration, which is relatively long. One half of the guard interval is used as conventional guard time to avoid inter-symbol interference between successive OFDM symbols.

The other half is used for transmit pulse shaping in order to decrease out-of-band radiation.

III. DME/TACAN SIGNALS

The basic DME/TACAN signal consists of two Gaussian-shaped pulses with an inter-pulse interval Δt of either 12 μs (X-mode) or 36 μs (Y-mode). In this paper, only the DME/TACAN signal in X-mode is of interest, which can be expressed as [4]

$$d(t) = e^{-\frac{\alpha}{2}t^2} + e^{-\frac{\alpha}{2}(t-\Delta t)^2} . \tag{1}$$

The parameter $\alpha = 4.5 \cdot 10^{11} s^{-2}$ is set such that the pulse width is 3.5 μs. In order to simulate the impact of DME/TACAN ground stations on a B-AMC system, the interference model outlined in [5] is adopted. In this model, the DME signal is modulated onto carrier frequencies on the left and the right of the OFDM system, i.e., ± 0.5 MHz, ± 1.5 MHz,..., with the center frequency of the OFDM system assumed at 0 Hz. The interference signal at the OFDM receiver can be considered as the superposition of N_{dme} contributing transmitters from DME stations operating in the same or different DME channels. The resulting interference signal can be expressed as

$$i(t) = \sum_{l=1}^{N_{\mathrm{dme}}} \sum_{p=1}^{N_l} A_l d(t - t_{l,p}) e^{j2\pi f_{c,l}t + j\varphi_l} , \tag{2}$$

where N_{dme} is the number of DME stations, N_l, $l = 1, \ldots, N_{\mathrm{dme}}$ represent the number of pulse pairs in the considered time interval for the lth DME station, A_l denotes the peak amplitude of the lth DME signal, $t_{l,p}$, $p = 1, \ldots, N_l$ are the starting times of the N_l pulse pairs of the lth DME station, and φ_l represents the phase of lth DME signal, which is uniformly distributed on $(-\pi, \pi]$.

IV. DME SIGNAL MITIGATION BY LATTICE-BASED CONSTELLATIONS

Signal space diversity or modulation diversity has been proved to provide high diversity order over fading channels [7], [8]. The diversity encoder of this method applies a unitary transform or rotation matrix $\mathbf{G}_M$ over the real or complex numbers to rotate a vector of information symbol $\mathbf{s}$ in the M-dimensional space, where M is the length of the information sequence. The resulting information symbol $\mathbf{x} = \mathbf{G}_M\mathbf{s}$ belongs to an M-dimensional signal set which has the property that each point is uniquely determined by any of its components which allows for retrieving it if some of its components are lost in a deep fade. Moreover, the transform leaves the Euclidean distance between any two information vectors unchanged. However, it modifies the distribution of the Euclidean distance over the components of the information vector and therefore introduces signal space diversity. Constructing optimum unitary transformations have been discussed in several papers [8]–[10]. The unitary transformations in [10] are the general case of the transformation in [9], and have a larger minimum product distance than the transformations

in [8]. The fully diverse unitary transformations can be represented as [10]:

$$\mathbf{G}_M = \mathbf{W}_M^H \mathbf{D}_\theta , \tag{3}$$

where $\mathbf{W}_M$ is the $M \times M$ discrete Fourier transform (DFT) matrix, $\mathbf{W}_M^H$ is its Hermitian transpose (IDFT), and

$$\mathbf{D}_\theta = \mathrm{diag}\left(1, \theta^{\frac{1}{M}}, \ldots, \theta^{\frac{M-1}{M}}\right) , \tag{4}$$

where θ is chosen algebraically to guarantee the full diversity of the rotation [10].

In Fig. 1, we show the proposed lattice encoder, which is capable of mitigating the DME signal. A block $\mathbf{S}$ of N_s input information symbols from the discrete alphabet $\mathcal{A}$, which is a QAM constellation normalized to unit power, is subdivided into L ($L = N_s/M$) subblocks. These subblocks are encoded into lattice code vectors X_l, $l = 1, \ldots, L$. Afterward, these code vectors are concatenated, then interleaved to form a transmitted codeword $\mathbf{C}$, where $\mathbf{C} = [C_0, C_1, \ldots, C_{N_s-1}]^T$. We adopted the same B-AMC system OFDM parameters as [1], where $N_s = 48$ represents the number of used subcarriers and $N = 64$ is the FFT size. At the receiver front-
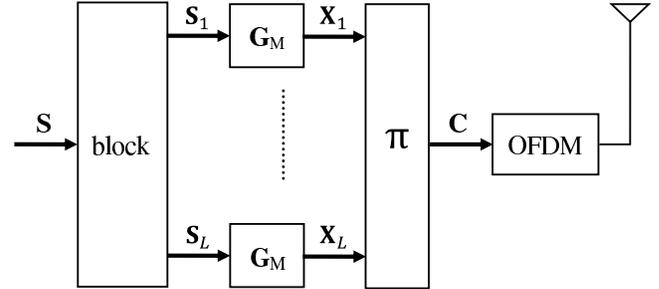

Fig. 1. Proposed lattice code structure for L-DACS1

end, the received signal consists of the desired OFDM signal, an additive white Gaussian noise (AWGN) component, and a DME interference contribution. When sampling the received signal with the sampling frequency of the OFDM system, an aliasing effect is observed from the DME signal spectrum which introduces additional interference within the OFDM spectrum. To circumvent this problem, an anti-aliasing filter in combination with oversampling is proposed [5]. Assuming perfect synchronization, the oversampled received signal is given by

$$r_k^{ov} = c_k^{ov} + z_k^{ov} + i_k^{ov}, \ k = 0, \ldots, VN - 1 , \tag{5}$$

where V denotes the oversampling factor, the samples c_k^{ov}, z_k^{ov}, and i_k^{ov} represent the desired OFDM signal, the oversampled AWGN, and the DME interfering signal, respectively.

The transmitted code components $\{C_n\}_{n=0}^{N_s-1}$ are recovered from the oversampled received sequence $\{r_k^{ov}[k]\}_{k=0}^{VN-1}$ by means of an FFT with size increased to VN in accordance to the oversampling factor, as follows:

$$\begin{aligned} R_n &= \frac{1}{\sqrt{VN}} \sum_{k=0}^{VN-1} r_k^{ov} e^{\frac{j2\pi kn}{VN}} \\ &= C_n + Z_n + I_n, \ n = 8, \ldots, 55 , \end{aligned} \tag{6}$$

where C_n is the transmitted lattice code component, Z_n is once again AWGN, and I_n is the FFT of the DME signal.

For the considered B-AMC system, the relevant subcarriers are selected, i.e., $n = 8, \ldots, 55$. The de-interleaved subcarriers are subdivided into L received lattice code vectors $\mathbf{R}_l$, $l = 1, \ldots, L$. The universal lattice decoding algorithm (sphere decoder) [11] can be used to decode the received vector $\mathbf{R}_l$. The sphere decoder takes advantage of the lattice structure of the received signals in maximum-likelihood fashion, i.e.,

$$\tilde{\mathbf{S}}_l = \arg \min \left\{ \left| \mathbf{R}_l - \mathbf{G}_M \mathbf{S}_l \right|^2 \right\}, \ l = 1, \ldots, L. \quad (7)$$

It applies the QR factorization to the received lattice matrix $\mathbf{G}_M = \mathbf{W}_M^H \mathbf{D}_\theta$, then searches for the closest lattice points to the received signal which are enclosed in a sphere of radius ρ centered at the received signal:

$$\left| \mathbf{R}_l - \mathbf{G}_M \mathbf{S}_l \right|^2 < \rho \quad (8)$$

$$\left| \mathbf{W}_M \mathbf{R}_l - \mathbf{W}_M \mathbf{W}_M^H \mathbf{D}_\theta \mathbf{S}_l \right|^2 = \left| \dot{\mathbf{R}}_l - \mathbf{D}_\theta \mathbf{S}_l \right|^2 < \rho \ .$$

We observe form (8) that multiplying the received vector $\mathbf{R}_l$ by $\mathbf{W}_M$ will make the interference contribution subject to a unitary transform, defined by the DFT matrix $\mathbf{W}_M$. This gives us a chance to mitigate and modify the DME signal spectrum in frequency domain, where the occurrence of DME signals can simply be detected. To illustrate the advantages of employing a lattice encoder followed by a random subcarrier interleaver at the B-AMC transmitter, we have considered a severe interference scenario described in [6]. In such a scenario, the B-AMC system is operating at 995.5 MHz and there are two interferers with a power up to -74 dBm in the channel at a $+0.5$ MHz offset to the B-AMC center frequency. In addition, a strong interferer is present in the channel at a -0.5 MHz offset to the B-AMC center frequency with a power of -67.9 dBm. The pulse rates of the interferers superimpose such that almost every OFDM symbol is affected by at least one pulse pair.

Figure 2 depicts the power spectrum of the received interfering signal (DME signal and noise) before and after the lattice decoder with unitary transformation by $\mathbf{G}_{24}$. The interfering signals are randomly generated for 1500 OFDM frames and the resulting power spectra[1] are averaged over all trials. We can see that, the outer subcarriers are subject to high interference power, which limits and deteriorates the performance of the B-AMC system. When lattice decoding is considered, the interference is averaged out over all used subcarriers, which make the system more robust against DME signals.

V. INTERFERENCE MITIGATION BY SUBCARRIER CLIPPING

Employing a lattice signal set followed by interleaver does not offer any interference mitigation. It averages out the interference power over all used subcarriers. However, in this

[1] The 'power spectrum' relates to the chosen symbol duration, i.e., for the figures, we treat the impulsive disturbance as stationary, which is, of course, not the case.
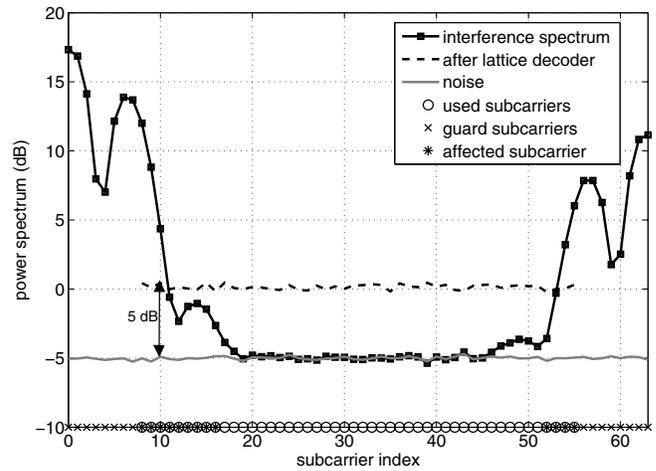

Fig. 2. Spectrum of interfering signal before and after lattice decoder

section, we propose a simple clipping method for interference mitigation in the frequency domain, where the affected subcarriers are known and the presence of a DME signal can easily be detected. The DME pulse detection is applied to the guard subcarriers at each side of the spectrum. At these subcarriers, the interference power level can be measured and, accordingly, the presence of DME interference can be detected.

A. Subcarrier Clipping

The interference mitigation scheme proposed in [6] applies an erasure decoding strategy that sets the unreliable information on the affected subcarriers to zero when the estimated SINR goes below a certain threshold. Unlike this technique, our proposed technique applies subcarrier clipping to the received lattice encoded symbols. The amplitudes of the received signals at the outer subcarriers (severely impaired by DME interference) are reduced to a certain thresholds T_n^{clip} when their amplitude exceeds T_n^{clip}. The clipping operation yields the clipped received signal as follows:

$$R_n^{\text{clip}} = \left\{ \begin{array}{ll} R_n \, , & \left| R_n \right| < T_n^{\text{clip}} \, , \\ T_n^{\text{clip}} e^{j \arg(R_n)} \, , & \left| R_n \right| \geq T_n^{\text{clip}} \, . \end{array} \right. \quad (9)$$

It is clear that not only the interference signal but the noise and the desired signal are affected by clipping as well. To keep the clipping impact on the useful signal at an acceptable level, the clipping thresholds T_n^{clip} have to be optimized as a trade-off between the achieved reduction of interference power and the impact on the desired signal. To apply clipping efficiently, the clipping operation is only applied to the subcarriers that are impaired by strong interference, i.e., $n = 8 \ldots, 16, 52, \ldots, 55$ (see Fig. 2). Moreover, the clipping operation is applied only when a DME signal is detected within the OFDM symbol.

B. Clipping Thresholds

In order to determine the optimum clipping thresholds of the outer subcarriers, the SINR after clipping operation should be maximized. The output signal after clipping can be represented

as the sum of a useful scaled replica of the desired signal and a nonlinear distortion [12], expressed by:

$$R_n^{\text{clip}} = \underbrace{\eta C_n}_{\substack{\text{useful} \\ \text{part}}} + \underbrace{W_n}_{\substack{\text{distorted} \\ \text{part}}} \ , \ n = 8, \ldots, 16, 52, \ldots, 55 \ , \quad (10)$$

where η is a scaling factor that represents the attenuation of the desired signal due to clipping. The scaling factor η is chosen such that the useful signal is uncorrelated with the noise process W_n, i.e., $E[W_n C_n^*] = 0$. The SINR after the clipping operation at the nth subcarrier can be expressed as

$$\text{SINR}(n) = \frac{E[|\eta C_n|^2]}{E[|R_n^{\text{clip}} - \eta C_n|^2]} = \frac{\eta^2}{E_{\text{out}} - \eta^2} \ , \quad (11)$$

where $E_{\text{out}} = E[|R_n^{\text{clip}}|^2]$ represents the total signal power at the nth subcarrier after clipping. The analytical derivation of η, E_{out}, and the optimum threshold for pulse clipping were considered in [12] for an impulsive noise environment. Since the probability distribution of the DME interference is significantly more complex, this approach cannot easily be extended to DME interference. Hence, the optimal thresholds of subcarriers clipping are determined by means of simulations for the considered DME interference scenario.

In these simulations, a B-AMC system employing the lattice coding is assumed. All OFDM symbols within one frame are used for transmitting QPSK modulated data coded with a rate $1/2$ convolutional code (CC). The optimization procedure is evaluated for the SNR region 0 to 5 dB. The average received power of the OFDM signal is normalized to 1 (0 dB). For the AWGN channel, the decoding of lattice codes can be performed by zero forcing such as lattice reduction-aided zero forcing [13]. Moreover, the DME pulse detection has been carried out in frequency domain using the guard subcarriers. In addition, subcarrier clipping is only applied when DME pulses are detected. The appropriate clipping thresholds are obtained for all affected subcarriers, i.e., $n = 8, \ldots, 16, 52, \ldots, 55$. For every clipped subcarrier, the corresponding interference contribution is added, and then the SINR curve versus clipping threshold is obtained.

In Fig. 3, the SINR curves after subcarrier clipping versus the threshold are shown for SNR=5 dB. Here, we only see the SINR results for the four low subcarriers. It is clear that the SINR curve increases with the threshold until it reaches the maximum achievable value. Afterward, the curve decreases to reach the value without clipping. Moreover, from the four curves, we note that as the interference power increases the optimum threshold decreases to keep the power of interference at a minimum value. To verify the choice of the thresholds, the spectrum of the interference (resulting from DME signal and noise) after subcarrier clipping is shown in Fig. 4. The clipping operations are applied at the first nine and the last four subcarriers. The figure also depicts the appropriate clipping threshold curve obtained by simulating SINR after clipping. With this choice of the thresholds, the impact of interference is reduced by 4 dB. The remaining gap (1 dB) between the interference power after subcarrier clipping and the interference-free case
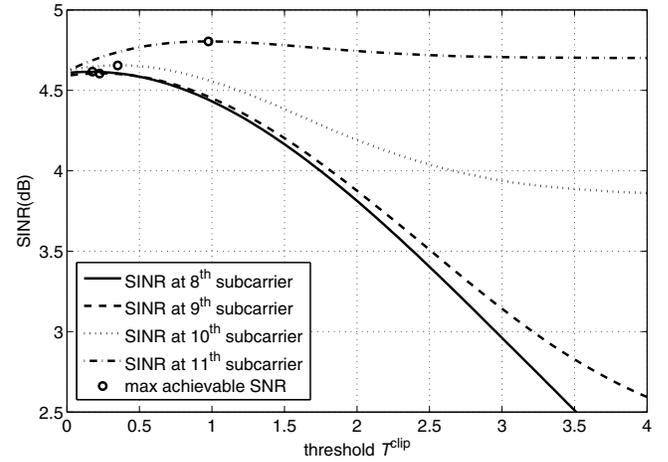

Fig. 3. Optimal clipping threshold T^{clip} at an SNR of 5 dB

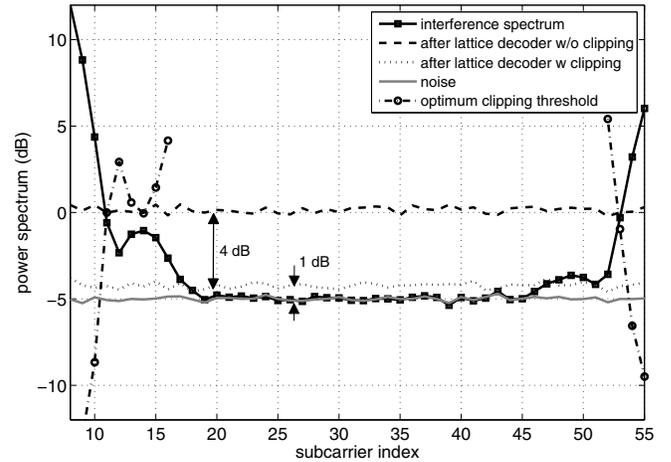is explained by the impact of subcarrier clipping on the desired signal.

Fig. 4. Spectrum of interfering signal after subcarrier clipping at an SNR of 5 dB

VI. SIMULATION RESULTS

The performance of the B-MAC system employing lattice coding is simulated and compared in terms of the bit-error ratio (BER) with pulse blanking, and CC erasure decoding. The data symbols are QPSK modulated with a $(133, 171)$ CC of rate $1/2$. To improve the correcting capability of the CC, a random interleaver to interleave all encoded bits within an OFDM frame is introduced as discussed in [6]. A lattice signal set with unitary transformation $\mathbf{G}_{24}$ is considered.

Figure 5 depicts the BER performance of the B-AMC system versus the SNR over an AWGN channel. The interference-free bound is given as a reference. As it can be seen, without applying any interference mitigation techniques, the performance after introducing the lattice coding improves the performance of the B-AMC system. Furthermore, the performance of the lattice coding with subcarrier clipping is

superior to the other mitigation techniques. At a BER of 10^{-4}, the proposed mitigation technique provides about 2 dB and 1 dB performance improvements over pulse blanking [5] and CC erasure decoding [6], respectively. The remaining gap (1 dB) between the interference-free case and the proposed subcarrier clipping method is due to clipping the desired signal. The per-
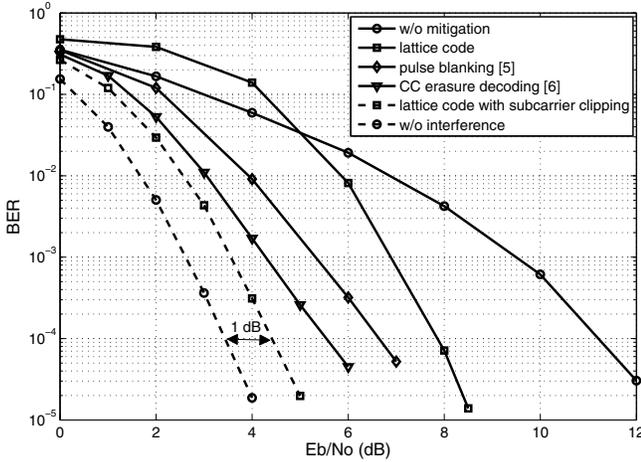

Fig. 5.   BER performance over AWGN channel

formance of the proposed interference mitigation technique is simulated in an aeronautical channel environment. Propagation conditions of an en-route flight can be modeled as one strong line-of-sight path with a Rice factor of 15 dB, and two reflected paths with a delay of $\tau_1 = 0.3$ μs and $\tau_2 = 15$ μs. In addition, a Doppler shift of 1250 Hz is considered, which corresponds to a velocity of 1360 km/h. Due to the strong LOS component, the channel behavior is expected to be similar to AWGN. Figure 6 depicts the performance of the proposed subcarrier clipping technique for different lattice code dimensions. For unclipped ones, the BER curves for the lattice codes at high SNR show that the performance is slightly worse when the lattice code dimension is decreased. This means that the ability of the lattice code to uniformly average the interference power is decreased as the code dimension is decreased. With clipping, the BER performances are not sensitive to the lattice code dimension.

VII. Conclusion

In this work, a DME interference suppression for OFDM based inlay systems is considered. Using a lattice signal set, the DME mitigation problem is moved from the time domain into the frequency domain, where a simple clipping method has been introduced. It has been confirmed by means of simulation that the proposed clipping method is capable of considerably reducing the impact of DME interference. Furthermore, the simulation in a realistic interference scenario has shown that the proposed approach provides better BER performance than the B-AMC system's mitigation techniques.
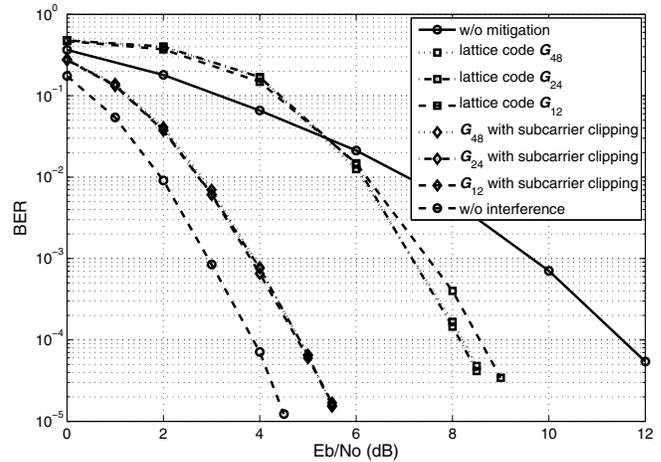
Acknowledgment

Fig. 6.   BER performance over en-route channel

References

[1] M. Schnell, S. Brandes, S. Gligorevic, C. H. Rokitansky, M. Ehammer, Th. Gräupl, C. Rihacek, and M. Sajatovic, "B-AMC - Broadband Aeronautical Multi-carrier Communications," *8th Integrated Communications, Navigation, and Surveillance (ICNS) Conference*, Bethesda, MD, USA, May 2008.

[2] C. H. Rokitansky, M. Ehammer, T. Gräupl, S. Brandes, S. Gligorevic, M. Schnell, C. Rihacek, and M. Sajatovic, "B-AMC - Aeronautical Broadband Communication in the L- band," *First CEAS European Air and Space Conference*, Berlin, Germany, Sept. 2007.

[3] S. Brandes, I. Cosovic, and M. Schnell, "Reduction of Out-of-Band Radiation in OFDM Systems by Insertion of Cancellation Carriers," *IEEE Communications Letters*, vol. 10, no. 6, pp. 420-422, June 2006.

[4] G. X. Gao, "DME/TACAN Interference and its Mitigation in L5/E5 Bands," in *ION Institute of Navigation Global Navigation Satellite Systems Conference*, Fort Worth, TX, USA, Sept. 2007.

[5] S. Brandes and M. Schnell, "Interference Mitigation for the Future Aeronautical L-Band Communication System," in *7th International Workshop on Multi-Carrier Systems & Solutions (MC-SS 2009)*, Herrsching, Germany, Ed. Springer, pp. 375-384, May 2009.

[6] M. Schnell, S. Brandes, S. Gligorevic, M. Walter, C. Rihacek, M. Sajatovic, and B. Haindl, "Interference Mitigation for Broadband L-DACS," in *27th Digital Avionics Systems Conference (DASC)*, St. Paul, MN, USA, Oct. 2008.

[7] K. Boullé and J. C. Belfiore, "Modulation Schemes Designed for the Rayleigh Fading Channel," in *Proc. Conf. Informotion Science and Systems*, Princeton, NJ, pp. 288-293, Mar. 1992.

[8] J. Boutros and E. Viterbo, "Signal Space Diversity: A Power and Bandwidth Efficient Diversity Technique for the Rayleigh Fading Channel," *IEEE Trans. Inform. Theory*, vol. 44, pp. 1453-1467, July 1998.

[9] X. Giraud, E. Boutillon, and J. C. Belfiore, "Algebraic Tools to Build Modulation Schemes for Fading Channels," *IEEE Trans. Info. Theory*, vol. 43, no. 3, pp. 938-952, May 1997.

[10] M. O. Damen, H. El Gamal, and N. C. Beaulieu, "Systematic Construction of Algebraic Full Diversity Constellations," *IEEE Trans. Inf. Theory*, vol. 49, no. 12, pp. 3344-3349, Dec. 2003.

[11] E. Viterbo and E. Biglieri, "A Universal Lattice Decoder," in *GRETSI 14-éme Colloque*, Juan-les-Pins, France, Sept. 1993.

[12] S. V. Zhidkov, "Performance Analysis and Optimization of OFDM Receiver With Blanking Nonlinearity in Impulsive Noise Environment," *IEEE Transactions on Vehicular Technology*, vol. 55, no. 1, pp. 234-242, Jan. 2006.

[13] D. Wübben, R. Böhnke, V. Kühn, and K. D. Kammeyer, "Near-maximum-likelihood Detection of MIMO Systems using MMSE-based Lattice-reduction," in *Proc. IEEE International Conference on Communications*, Paris, France, pp. 798-802, June 2004.